Internal Dynamics of Cyclohexanol and the Cyclohexanol-Water Adduct

Marcos Juanes,[a] Weixing Li,[b] Lorenzo Spada,[b,c] Luca Evangelisti,[b,]* Alberto Lesarri,[a,]*
Walther Caminati[b]

[a]Departamento de Química Física y Química Inorgánica, Facultad de Ciencias, Universidad de Valladolid, E-47011 Valladolid, Spain.
[b]Dipartimento di Chimica "Giacomo Ciamician" dell'Università, Via Selmi 2, I-40126 Bologna, Italy.
[c]Present Address: Scuola Normale Superiore, Piazza dei Cavalieri 7, 56126 Pisa (Italy)

Corresponding Authors:

*Luca Evangelisti, Email: luca.evangelisti6@unibo.it, Ph: 0039-051-2099480

*Alberto Lesarri, Email: lesarri@qf.uva.es, Ph: 0034-983-185895

ABSTRACT: Two conformers of cyclohexanol and the cyclohexanol-water adduct have been characterized in a jet expansion using rotational spectroscopy. In the gas phase cyclohexanol adopts an equatorial position for the hydroxyl group, with the two conformers differing in the orientation of the hydroxylic hydrogen, either *gauche* or *trans* with respect to the aliphatic hydrogen at C(1). The transitions of the *gauche* conformer are split into two component lines due to the tunneling effect of the O-H internal rotation, which connects two equivalent *gauche* minima. The tunneling splitting in the vibrational ground state has been determined to be ΔE_{0+0-} =52(2) GHz. From this splitting the inversion barriers connecting the two equivalent *gauche* conformers has been determined using a flexible model to be B_2= 376.6 cm^{-1}. A single isomer is detected for the cyclohexanol-water dimer, in which the water molecule acts as proton donor to the ring oxygen. The presence of torsional tunneling in the adduct suggests a concerted large-amplitude-motion in which the internal rotation in the ring is accompanied by a torsion of the water molecule, to produce an equivalent enantiomer. The torsional tunneling in the adduct is reduced to ΔE_{0+0-} =32.7(4) GHz resulting in a barrier B_2 = 494 cm^{-1} as pointed out by using the flexible model.

Introduction

Alcohols, R-OH, are characterized by three energy minima upon a 360° internal rotation of the hydroxyl group. Depending on the symmetry of the R group, these three minima can be: (*i*) energetically equivalent to each other; (*ii*) two of them equivalent, but different from the third one; (*iii*) all of them with different energy values. In the last two cases a conformational equilibrium is obtained, while in the first cases tunneling and mixing of wavefunctions make the pattern of rotational levels very difficult to be interpreted. Further conformational species can appear when R has a high flexibility.

Rotational spectroscopy is a technique especially suitable to investigate conformational equilibria and to unveil tunneling effects in case of equivalent minima, which can also be analyzed to the formation of intermolecular clusters, in particular hydrates.

In methanol and *tert*-butanol the C_3 symmetry of R allows only one conformer to exist, but their rotational spectra have been found extremely difficult to analyze because of multiple tunneling effects.[1,2] Conversely, in ethanol and *iso*-propanol the C_s symmetry of R leads to the detection of the rotational spectra of the *trans* and *gauche* conformers, with a tunneling motion connecting the two equivalent *gauche* forms.[3,4] The R chain in *n*-propyl alcohol is flexible and it can adopt either a *trans* (with C_s symmetry) or a *gauche* shape (with C_1 symmetry). As in ethyl alcohol, *trans* generates, upon rotation of the hydroxyl group, a *trans-trans* and a *trans-gauche* (tunnelling) species (labelled *Tt* and *Tg*). *Gauche* generates, upon rotation of the hydroxyl group, three distinguished non-tunneling conformers, *Gt*, *Gg*, *Gg*'. All together, five conformers were assigned in the microwave spectrum.[5] For the larger *n*-pentan-2-ol and *n*-hexan-2-ol rotational spectroscopy has detected 5 and 14 conformers, respectively.[6]

Concerning cyclic alcohols, the rotational spectra of *gauche*-cyclopropanol[7] and of the *equatorial-trans* form of cyclobutanol[8] have been observed. The rotational spectrum of cyclopentanol is not reported. Finally, four conformers were assigned for 1-methylcyclohexanol,[9] denoted *Eg, Et, Ag, At* (*E* is the abbreviation of equatorial, and *A* is axial) For cyclohexanol ($C_6H_{12}O$) neither the monomer nor the water dimer have been reported. For this reason, we decided to study the conformational equilibria for the bare molecule and the hydrate using supersonic jet Fourier transform microwave spectroscopy.

Cyclohexanol ($C_6H_{12}O$) is an important feedstock in the polymer industry, as a precursor to nylons and various plasticizers. It is also used as a solvent. The chair form of the aliphatic ring is the most stable one. However, the orientation of the hydroxyl group gives rise to four possible isomers. The hydroxyl group may be attached in the equatorial (*E*) or axial (*A*) positions of the cyclohexyl ring. In both cases R has a C_s symmetry, and it can generate *trans* and *gauche* (doubly degenerated) species, for a total of four conformers. James et al.[10] concluded from the temperature dependence of the Raman spectra that in the ordered phases the equatorial isomer dominates the structure of the phase. Andre et al.[11] found that there is an equal distribution of axial and equatorial forms in the glassy phase. More recently Ibberson et al.[12] found that the cyclohexanol molecules adopt only equatorial shapes in crystal, by using high-resolution neutron diffraction of powder, synchrotron X-ray diffraction of powder and single-crystal X-ray diffraction techniques.

Adducts of alcohols with water are also quite important systems, with interesting motifs such as conformational equilibria, the play of donor/acceptor roles of water and alcohol, and puzzling internal dynamics, where the internal rotation of the hydroxyl group is often combined with the motions of water. Recent investigation these molecular systems concern the 1:1 adducts of water with *tert*-butyl alcohol,[13] *iso*-propyl alcohol,[14] *n*-propyl alcohol[15] and ethyl alcohol.[16]

Here we report the data for the adduct of water with a cyclic alcohol.

Experimental

Samples of $C_6H_{12}O$ were obtained commercially (Aldrich) and used without further purification. The rotational spectrum has been measured in two different laboratories:

a) Bologna. A COBRA-type[17] Fourier-transform microwave spectrometer[18] (FTMW) was used to cover the frequency range 6.5-18 GHz.[19] Helium at a stagnation pressure of ~0.3 MPa was passed over a container with $C_6H_{12}O$ under room temperature and expanded through a solenoid valve (Parker, Series 9, nozzle diameter 0.5 mm) into the Fabry-Pérot cavity. The gas-phase expansion formed a supersonic jet, cooling the molecules in their lowest vibrational state. The spectral line positions were determined after Fourier transformation of the time-domain signal with 8k data points, recorded with 100 ns sample intervals. Each rotational transition appears as doublets due to Doppler effect. The line positions are calculated as the arithmetic mean of the frequencies of the Doppler components. The estimated accuracy of the frequency measurements is better than 3 kHz. Lines separated by more than 7 kHz are resolvable.

b) Valladolid. The rotational spectrum has been recorded with a broadband direct-digital chirp-pulse FTMW spectrometer covering the frequency range 2-8 GHz, which follows Pate's design.[20] In this spectrometer a 5 μs chirp pulse created by an arbitrary waveform generator is amplified to 20 W and radiated perpendicular to the propagation of the jet expansion through a horn antenna. A molecular transient emission spanning 40 μs is then detected through a second horn, recorded with a digital oscilloscope and Fourier-transformed to the frequency domain. Sample preparation was similar to Bologna, with optimal conditions requiring backing pressures of ca. 0.4 MPa and neon as carrier gas. The accuracy of the frequency measurements is better than 15 kHz.

Theoretical calculations

The conformational equilibrium of $C_6H_{12}O$ is driven by the ring puckering, which can interconvert the axial or equatorial location of the OH group, and by the internal rotation of the hydroxyl group, which can generate *gauche* and *trans* orientations of the hydroxylic hydrogen with respect to the aliphatic hydrogen in C1. These two internal motions generate six energy minima, which correspond to four different conformers, labeled as, *Eg, Et, Ag, At* (*A*, *E*, *t* and *g* stand for *axial*, *equatorial*, *trans* and *gauche*). Each *gauche* form is doubly degenerated because of the two equivalent orientations of hydroxyl group around C-O bond. We performed ab initio calculations (MP2/6-311++G(d,p)[21]) to determine the optimized structures, relative energies, rotational and centrifugal distortion constants, and the electric dipole moment components for the four conformers. Vibrational frequency analysis confirmed further that all these conformers are stable energy minima. All theoretical data are summarized in Table 1.

For the $C_6H_{12}O$-water dimer we performed an initial molecular mechanics conformational search followed by re-optimization with ab initio and dispersion-corrected density-functional theory. Table 2 presents the two most stable hydrated structures, with energetic and structural predictions according to MP2/6-311++G(d,p) level of calculation. For comparison purposes additional calculations were performed using the B3LYP-D3 method. In both cases *Eg*-water and *Et*-water turned out to be the most stable isomers of the hydrate.

Rotational spectra

Guided by the predicted rotational constants in Table 1, a few rotational transitions for the two equatorial *E*g and *E*t conformers were first assigned in the broadband spectrum in the range 2-8 GHz. More μ_a- and μ_c-type transitions for both conformers were then measured in the range 6-18.5 GHz using the cavity spectrometer. As illustrated in Figure 1, all the transitions for the *E*g conformer appeared as doublets because of the hydroxyl group internal rotation. These splittings led to the assignment of the pair of ground torsional states, denoted 0^+ and 0^-. Searches for plausible axial conformers were performed unsuccessfully. We rationalized that collisional mechanisms in the jet produce an efficient conformational relaxation into the global minimum, as observed empirically when the interconversion barrier between equilibrium minima is below $2kT$.[22] Evidence for this argument comes from the fact that the *Et/Eg* population ratio should be 0.34 according to a Boltzmann distribution, while the *Et/Eg*(0^+) spectra intensity ratio is lower, i.e., it is just 0.1 in the transition $3_{03} \leftarrow 2_{02}$. This implies the global minimum is more populated than expected.

All equatorial *trans* transitions were fitted with Watson's semirigid-rotor Hamiltonian, including quartic centrifugal distortion constants (I^r representation and *S* reduction).[23,24] For the *gauche* conformer, the tunneling splittings were fitted using a two-state torsion-rotation coupled Hamiltonian, including semirigid rotor terms for each torsional state ($\boldsymbol{H}_0^R, \boldsymbol{H}_1^R$), common centrifugal distortion ($\boldsymbol{H}^{CD}$), the torsional energy difference ΔE_{0+0-}, and Coriolis coupling terms F_{bc} and F_{ab} determined in the reduced axis system of Pickett, according to equations

$$\boldsymbol{H} = \begin{pmatrix} \boldsymbol{H}_0^R + \boldsymbol{H}^{CD} & \boldsymbol{H}_{int} \\ \boldsymbol{H}_{int} & \boldsymbol{H}_1^R + \boldsymbol{H}^{CD} + \Delta E_{0^+0^-} \end{pmatrix} \tag{1}$$

where the interaction term is expressed:

$$\boldsymbol{H}_{int} = F_{bc}\,(\boldsymbol{P_b P_c} + \boldsymbol{P_c P_b}) + F_{ab}\,(\boldsymbol{P_a P_b} + \boldsymbol{P_b P_a}) \tag{2}$$

where $\boldsymbol{P_\alpha}$ (α=a, b, c) represents angular momentum operators. The fitted spectroscopic constants for the two equatorial species are reported in Table 3. All experimental transition frequencies are given in Tables S1 and S2 (ESI).

The spectral measurements were extended to the monosubstituted ^{13}C and ^{18}O isotopic species in natural abundance for the most abundant *Eg* conformer, definitively confirming the spectral assignment. A single transition was observed for the near-symmetric $^{13}C(2)/^{13}C(6)$ and $^{13}C(3)/^{13}C(5)$ positions. The rotational parameters and transition frequencies for the minor isotopologues are in Tables S3-S8 (ESI).

Investigation of the monohydrated cyclohexanol-water dimer started with the ab initio predictions and the broadband spectrum. The spectral signature of an asymmetric rotor was then discovered, exhibiting torsional doublings similar to the parent species. Analysis of the spectrum required a two-state Hamiltonian, with the same Coriolis coupling terms as in the monomer. The assignment of water dimer was later confirmed by observation of the $H_2{}^{18}O$ cluster using an isotopically enriched water sample, as shown in Figure 2. The spectroscopic results for the dimer are collected in Tables 4 and S9 (ESI), while transition frequencies are presented in Tables S10-S11 (ESI).

Molecular Structure and Potential energy function of the OH group internal rotation

Molecules exhibiting large-amplitude motions cannot be described by rigid structural parameters but for the potential function controlling the intramolecular dynamics. In equatorial cyclohexanol the observation of isotopic species and the torsional energy difference ΔE_{0+0-} allows determining both the heavy-atom skeleton and the hydroxyl internal rotation potential function.

The skeleton of cyclohexanol was determined with the substitution and effective structures. The results are presented in Tables S12 and S13, where they are also compared with ab initio results.

The OH internal rotation potential function was calculated with the monodimensional flexible model of Meyer,[25] which allows the numerical calculation of the rotational and vibrational wave functions and eigenvalues (and then vibrational spacings). The internal rotation of the hydroxyl group, described by the dihedral angle HC-OH (τ), was first modelled using ab initio methods. The MP2/6-311++G(d,p) potential function of the equatorial conformer is represented by the red line in Figure 3. This function was parametrized as

$$V(\tau) = V_0 + V_1\cdot(1\text{-}\cos\tau) + V_2\cdot(1+\cos2\tau) + V_3\cdot(1+\cos3\tau) \qquad (3)$$

The values of the four parameters V_i, i= 0-3, are shown in Table 5. There also the energy barriers between the two gauche forms (B_2) and between the trans and the gauche form ($B_{t\to g}$), as well as the energy difference between the two conformers (E_t-E_g) are given. Guided by the theoretical calculations, we took into account the main structural relaxation parameters associated to the internal rotation, according to equations of the type:

$$S_i(\tau) = S^0{}_i + \Delta S_i(\tau) \qquad (4)$$

For a given parameter S, S^0 is the value at $\tau = 0$ while ΔS is its variation as a function of τ. All these values have been obtained from the *ab initio* geometries at the four critical points. Six structural relaxations have been taken into account for the model calculations. The corresponding detailed expressions, according to eq. (4), are given in the supporting information as Table S14 (ESI).

Meyer's model produced a reasonable reproduction of the torsional splitting by multiplying Eq (3) by a scale factor of 0.9 (the τ coordinate has been considered in the 2π cyclic range and solved into 61 mesh points). The barrier to the *gauche* ↔ *gauche* pathways (B_2) resulted to be 377 cm^{-1}, which is slightly larger than that in 1-methylcyclohexanol (356 cm^{-1}, and 320 cm^{-1} for *axial* and *equatorial* species, respectively) but lower than the *ab initio* result of 420.7 cm^{-1}. All these data are shown in Table 6. The resulting potential energy function is given in Figure 3 (black trace), together with the wavefunctions of the lower energy levels.

Water dimer geometry and dynamics

As expected a moderately strong O-H···O hydrogen bond will stabilize the adduct of cyclohexanol-water. However, the ab initio calculations did not offer a priori a clear structural prediction, as the two most stable dimer geometries (*Eg*-H_2O and *Et*-H_2O) in Table 2 are practically isoenergetic ($E_{Et\text{-H2O}} - E_{Eg\text{-H2O}}$ = 1.1 kJ mol^{-1}) using the MP2 method in combination with the 6-311++G(d,p) basis set. Additional calculations for two more isomers obtained from the conformational search (A_g-H_2O and E_{g2}-H_2O) in Table S15 (ESI) predicted larger relative energies. These structures were reoptimized with the dispersion-corrected B3LYP-D3 method for comparison purposes in the same Table.

The spectrum provided definitive experimental evidence of the geometry of the cluster and its internal dynamics. The determined rotational constants in Tables 4 and S9 (ESI) unequivocally confirm the detection of isomer *Eg*-H_2O, based on the most stable *gauche* monomer. The water molecule acts as proton donor to the oxygen lone pair at the ring, as in other aliphatic alcohols.[13-16] Interestingly, the tunneling effects in the dimer are evidence of a large-amplitude motion, which in principle could be related either to the internal rotation of the OH group of cyclohexanol or to the internal rotation of water around its C_2 axis. Tunnelling plittings associated to this last motion should be very small, because it would imply the breaking and reformation of a relatively strong O-H···O hydrogen bond with a high barrier between the two equivalent forms. In consequence, the cluster dynamics is most probably associated to the internal rotation of the hydroxyl group. The most reasonable scenario is a concerted motion involving the internal rotation of the OH group of cyclohexanol combined with the simultaneous rearrangement of the water molecule, as observed in tert-butyl-water[13] and isopropanol-water dimers.[14] The decrease in the torsional energy difference in the dimer (ΔE_{0+0-}= 32.7(4) < 52(2) GHz in the monomer) is consistent with this hypothesis.

Despite only two isotopic species were detected for the cyclohexanol-water dimer we estimated the hydrogen bond distance using an effective structure (Table S16, ESI) . The resulting value of $r(O\text{-}H_w)$=1.928(5) Å is slightly larger than the ab initio prediction (1.881 Å), but within the broad range observed for this interaction in crystal structures (1.40-2.18 Å).[28] The substitution coordinates of the water oxygen are calculated in Table S17 (ESI). A recent review offers information on other water clusters detected by rotational spectroscopy.[29]

Meyer's flexible model was utilized also to calculate the barrier to inversion between the two equivalent *Eg*-H_2O forms of the complex. The OH internal rotation should be described by a periodic function, but in this we can reasonably assume that the tunneling effects are produced 'locally' in the range of the HO-CC dihedral angle (τ) between ca. -120 and +120°. Then, the following double minimum potential can be used:

$$V(\tau) = B_2\,[1 - (\tau/\tau_0)^2]^2, \qquad (5)$$

B_2 is the barrier at $\tau = 0°$ and τ_0 is the equilibrium value of the inversion angle. Since we have only one data point, we fixed τ_0 at its *ab initio* value (63.3°). Guided by the *ab initio* structural differences between the energy minimum ($\tau = \tau_0$) and the transition state ($\tau = 0°$), we took into account the main structural relaxations, those of the three structural parameters indicated below, as a function of the leading parameter τ, according to the following expressions (see Fig. 4 for labelling):

$$\mathrm{H2O2\text{-}O1C1}/° = 180 - 27.9\cdot(\tau/\tau_0) \qquad (6)$$

$$\mathrm{H2O2O1}/° = 15.8 - 3.2\cdot(1\text{-}\cos 3\tau). \qquad (7)$$

$$R(O2\text{-}O1)/\text{Å} = 2.8485 + 0.0042\cdot(1-\cos 3\tau). \qquad (8)$$

The experimental splitting of 32.7 GHz is reproduced by a B_2 barrier of 494 cm^{-1}.

Discussion and Conclusions

We presented a rotational investigation on the internal dynamics of cyclohexanol and the adduct cyclohexanol-water. The conformational equilibria in cyclohexanol is displaced towards the two *gauche* and *trans* equatorial forms E_g and E_t. This observation contrasts with the case of 1-methylcyclohexanol,[9] where we succeeded in observing also the axial conformers. This fact suggests that the presence of a methyl group adjacent to the OH group decreases the energy differences between the axial and equatorial forms. The detection of tunneling doublings was instrumental for the evaluation of the potential function for the internal rotation of the hydroxyl group. The comparison of the B_2 potential energy barriers hindering the motion between the equivalent E_g forms is also interesting. The ab initio values are B_2 = 420 and 410 cm^{-1} for cyclohexanol and 1-methylcyclohexanol,[9] respectively. However, the experimental data suggest B_2 quite larger in cyclohexanol (377 cm^{-1}) than in 1-methylcyclohexanol (320 cm^{-1}). How to justify that? It can be argued that the presence of a methyl group in the carbon atom to which the hydroxyl is attached lowers the barrier to internal rotation of OH group in the section connecting the two *gauche* forms. By comparing the tunnelling splitting with the values in the case of other five alcohols, we found that the order of torsional energy differences ΔE_{0+0-} is as: Cyclopropanol < Isopropanol < Cyclohexanol < n-Propanol < Ethanol < 1-Methycyclohexanol (see Table 8). All of the alcohols have both *trans* and *gauche* conformers. For the first three alcohols the hydrogen atom is adjacent to the OH group, whereas for the latter alcohols an alkyl group is replacing the H atom.

Acknowledgment. We acknowledge Italian MIUR (PRIN project 2010ERFKXL_001) and the University of Bologna (RFO) for financial support. M.J and A.L. thank the MINECO for funds (CTQ2015-68148-C2-2-P). W. L. thanks the China Scholarships Council (CSC) for a scholarship. L. E. was supported by Marie Curie fellowship PIOF-GA-2012-328405. We acknowledge the CINECA award under the ISCRA initiative, for the availability of high performance computing resources and support**.**

†**Electronic Supplementary Information Available:** Electronic supplementary information (ESI) available: Tables S1–S17 with the completion of Ref. [17], transition frequencies, rotational parameters of the isotopic species, ab initio calculations, structural data and description of the structural relaxations taken into account in the flexible model calculation. See DOI: 10.1039/xxxxxxxxxxx.

Author Contributions

The manuscript was written through contributions of all authors. All authors have given approval to the final version of the manuscript. All authors contributed equally.

Figure 1. A typical rotational transition ($3_{03} \leftarrow 2_{02}$) of cyclohexanol recorded with the cavity spectrometer, showing two torsional tunneling components ($0^+/0^-$) for the equatorial *gauche* conformer (*Eg*) but a single component for the trans species (*Et*). Each transition is additionally doubled by the Doppler effect.

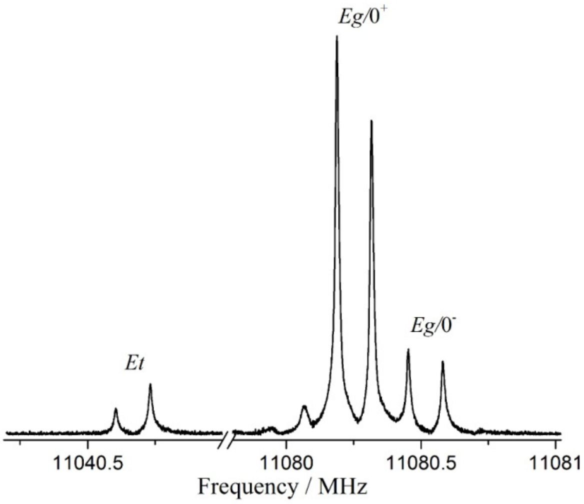

Figure 2. A section of the spectrum of cyclohexanol···$H_2{}^{16}O$ and cyclohexanol···$H_2{}^{18}O$ recorded with the broadband spectrometer, showing the isotopic shift caused by ^{18}O-water. The torsional splitting is observed only for the most intense $2_{0,2} \leftarrow 1_{0,1}$ transition.

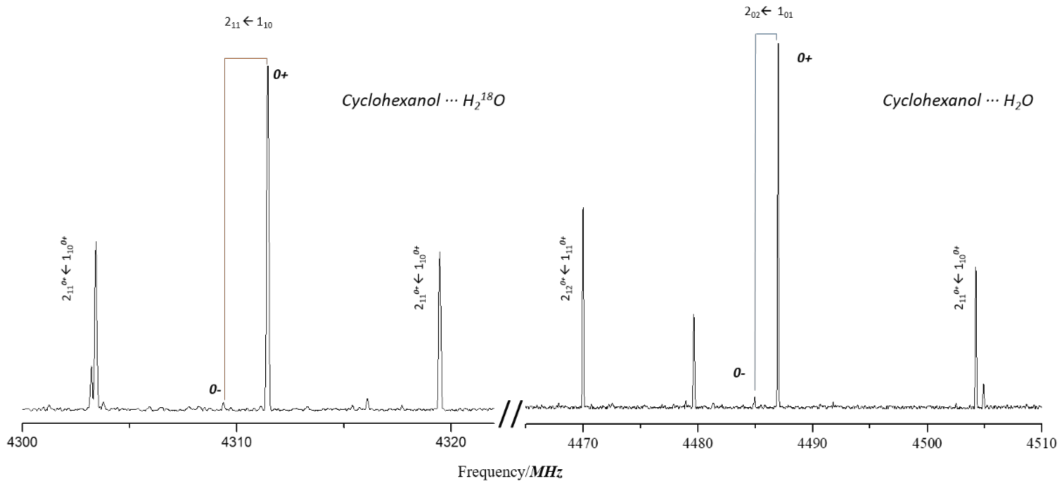

WRONG FIGURE!

Figure 3. *Ab initio* (red trace) and experimental (black trace) potential energy curves as a function of dihedral angle HC-OH (cm^{-1} vs degrees) when the OH group rotates around CO bond in the *equatorial* conformers. The wavefunctions of the lower states are also drawn on the right.

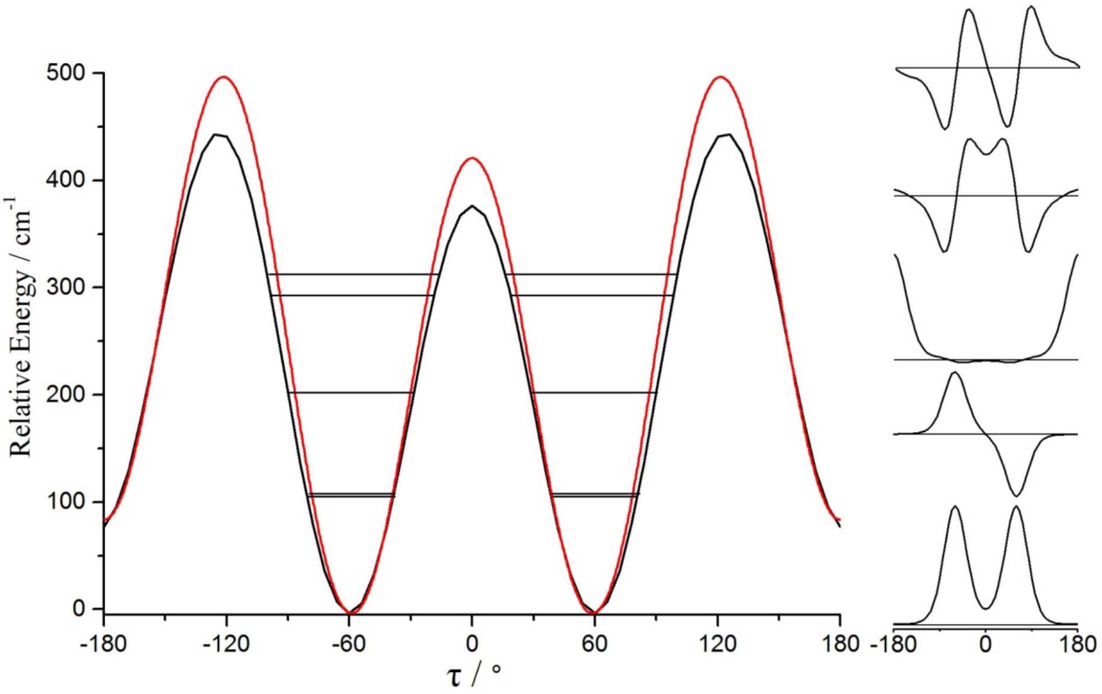

Fig. 4. Labeling of the atoms involved in the flexible model analysis of **Eg**-W-*GAI*. Hf indicates the "free" (not involved in the hydrogen bond) water hydrogen

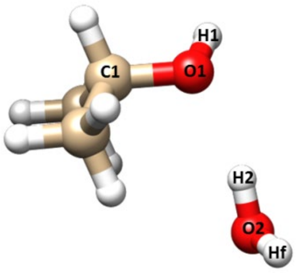

Table 1 Molecular structures, relative energies and spectroscopic predictions for the four conformers of cyclohexanol (MP2/6-311++G(d,p)).

	Eg	***Et***
	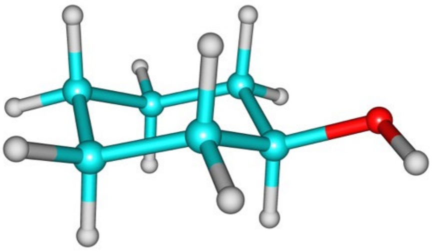	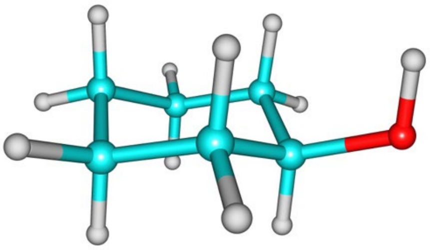
A,B,C/MHz	4309.1, 2238.5, 1617.8	4304.5, 2218.0, 1613.4
μ_a,μ_b,μ_c/D	0.5,1.5,1.0	1.4,0.0,1.4
$\Delta(E+\text{ZPE})$/ kJ mol^{-1}	0.00	0.96
ΔG/ kJ mol^{-1}	0.00	0.82
	Ag	***At***
	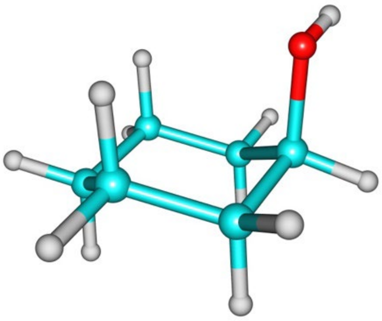	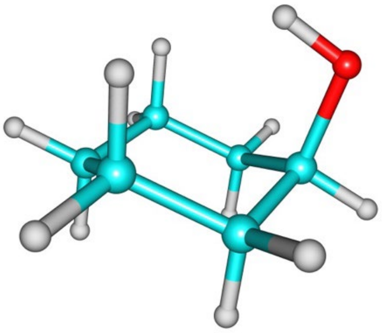
A,B,C/MHz	3556.0, 2671.7, 2006.3	3581.4, 2612.8, 1972.8
μ_a,μ_b,μ_c/D	0.5,1.5,0.2	1.2,0,1.6
$\Delta(E+\text{ZPE})$ / kJ mol^{-1}	1.78	5.73
ΔG / kJ mol^{-1}	1.97	5.57

Table 2 Molecular structures, relative energies and spectroscopic predictions of the most stable isomers of cyclohexanol-water (MP2/6-311++G(d,p)).

	$Eg \cdots H_2O$	**$Et \cdots H_2O$**
	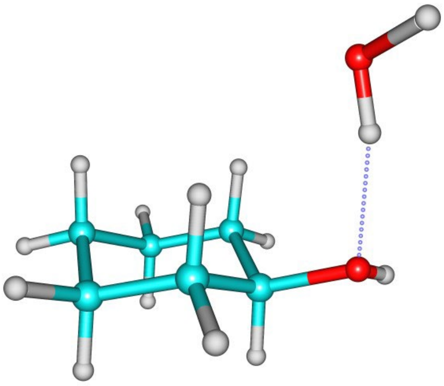	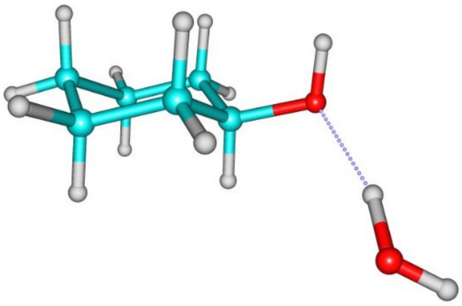
A,B,C/MHz	2553.7, 1166.6, 1139.8	3183.0, 1071.1, 889.1
μ_a,μ_b,μ_c/D	1.8, 0.6, 0.9	1.4, 0.9, 1.9
$\Delta(E+\mathrm{ZPE})$ / kJ mol^{-1}	0.0	1.1
ΔG / kJ mol^{-1}	0.1	0.0
ΔE_B / kJ mol^{-1}	-22.9	-23.3

Table 3 Experimental spectroscopic parameters of the two equatorial conformers of cyclohexanol.

	Cyclohexanol		
	Eg		***Et***
	0^+	0^-	
A/MHz	4295.7884(8)[a]	4293.3876(7)	4288.1884(5)
B/MHz	2231.4842(4)	2231.7890(5)	2215.7086(6)
C/MHz	1612.4343(5)	1612.4672(5)	1609.2335(5)
D_J/kHz	0.116(9)		0.120(12)
D_{JK}/kHz	0.25(3)		0.312(38)
D_K/kHz	0.52(9)		
d_1/kHz	-0.029(6)		-0.0422(94)
d_2/kHz	-0.006(5)		-0.0171(55)
ΔE_{0+0-}/GHz	52(2)		
F_{ab}/MHz	11.16(2)		
F_{bc} /MHz	4.57(7)		
σ[b]/kHz	1.75		2.7
N[c]	53		27

[a] Errors in parenthesis are expressed in units of the last digit. [b] Standard deviation of the fit. [c] Number of fitted transitions.

Table 4 Experimental spectroscopic parameters of the observed conformer, E_g-cyclohexanol-water.

	Cyclohexanol ··· H_2O	
	0^+	0^-
A/MHz	2555.2943(21)d	2556.2312(50)
B/MHz	1130.35883(48)	1129.94502(59)
C/MHz	1113.24155(43)	1112.60936(75)
D_J/kHz	-1.3293(57)	
D_{JK}/kHz	2.75(13)	
D_K/kHz	-6.87(24)	
d_1/Hz	0.1375(26)	
d_2/Hz	0.0449(42)	
ΔE_{0+0-}/GHz	32.7(4)	
F_{ab}/MHz	15.4(2)	
F_{bc} /MHz	5.76(5)	
σ^b/kHz	7.2	
N^c	74	

[a]Errors in parenthesis are expressed in units of the last digit. [b]Standard deviation of the fit. [c]Number of fitted transitions.

Table 5 MP2/6-311++G(d,p) values of the V_i coefficients in Eq. (3) for the internal rotation potential function. The energy values at the critical points, relative to the *gauche* energy minimum, are also given.

V_0/cm^{-1}	V_1/cm^{-1}	V_2/cm^{-1}	V_3/cm^{-1}	B_2/cm^{-1}	E_t-E_g/cm^{-1}	$B_{t\rightarrow g}$/cm^{-1}
-32.44	54.0	4.0	222.6	420.7	83.5	496.5

Table 6 Results of the flexible model calculations for equatorial cyclohexanol.

Tunneling splittings		
	Obs.	Calc.
ΔE_{0+0-}/ GHz	52.2	52.2
Parameters:		
Scale factor f (fitted)	0.895	
Barrier B_2 (extrapolated) /cm^{-1}	377	

Table 7. Comparison of the *cis*-inversion tunnelling splitting energies ΔE_{0+0-} of alcohols.

Species	ΔE_{0+0-}/ GHz
Cyclopropanol	4.1[a]
Isopropanol	46.8[b]
Cyclohexanol	52.2[c]
n-Propanol	91[d]
Ethanol	96.7[e]
1-Methylcyclohexanol	102.5/103[f,g]

[a] Ref. 7. [b] Ref. 4. [c] This work. [d] Ref. 5. [e] Ref. 3. [f] The values are for *axial* and *equatorial* forms, respectively. [g] Ref. 9.

REFERENCES

1) See, for example, O. I. Baskarov and M.A.O. Pashaev, *J. Mol. Spectrosc.* 1991, **151**, 282-291, and references therein.

2) E.A. Cohen, B.J. Drouin, E.A. Valenzuela, R.C: Woods, W. Caminati, A. Maris and S. Melandri, *J. Mol. Spectrosc*. 2010, **260**, 77–83.

3) R.K. Kakar and C.R. Quade, *J. Chem. Phys*. 1980, **72**, 4300-4307.

4) See, for example, E. Hirota and Y. Kawashima, *J. Mol. Spectrosc.* 2001, **207**, 243-253; and ref.s therein.

5) Z. Kisiel, O. Dorosh, A. Maeda, I.R. Medvedev, F.C. De Lucia, E. Herbst, B.J. Drouin, J.C: Pearson, and S.T. Shipman, *Phys. Chem. Chem. Phys*. 2010, **12**, 8329-8339.

6) M.J. Tubergen, A.R. Conrad, R.E. III Chavez, I. Hwang, R.D. Suenram, J.J. Pajski, and B.H. Pate, *J. Mol. Spectrosc*. 2008, **251**, 330–338.

7) J.N. Macdonald, D. Norbury and J. Sheridan, *J. Chem. Soc., Faraday Trans.* 2 1978, **74**, 1365-1375.

8) W. Lin, A. Ganguly, A.J. Minei, G.L. Lindeke, W.C. Pringle, S.E. Novick and J.R. Durig, *J. Mol. Struct.* 2009, **992**, 83–87.

9) W. Li, L. Spada, L. Evangelisti, and W. Caminati, *J. Phys. Chem. A*, 2016, **120**, 4338-4342.

10) D. W. James, H. F. Shurvell and R. M. Parry, *J. Raman Spectrosc.* 1976, **5**, 201-209.

11) D. Andre, D. Ceccaldi and H. Szwarc, *J. Phys. (France)*, 1984, **45**, 731-737.

12) R. M. Ibberson, S. Parsons, D. R. Allan and A. M. T. Bellc, *Acta Cryst.* 2008, **B64**, 573–582.

13) L. Evangelisti and W. Caminati, *Phys. Chem. Chem. Phys*. 2010, **12**, 14433-14441.

14) L. Evangelisti, Q. Gou, G. Feng, W. Caminati, G. J. Mead, I. A. Finneran, P. Brandon Carroll and G. A. Blake, *Phys. Chem. Chem. Phys.* 2017, **19**, 568–573.

15) G. J. Mead, E. R. Alonso, I. A. Finneran, P. B. Carroll, G. A. Blake, *J. Mol. Spectrosc*. 2017, **335**, 68 – 73.

16) I. A. Finneran, P. B. Carroll, M. A. Allodia, G. A. Blake, ***Phys. Chem. Chem. Phys.***, 2015,**17**, 24210-24214.

17) J.-U. Grabow, W. Stahl and H. Dreizler, *Rev. Sci. Instrum.* 1996, **67**, 4072−4084.

18) T. J. Balle and W. H. Flygare, *Rev. Sci. Instrum.* 1981, **52**, 33−45.

19) W. Caminati, A. Millemaggi, J. L. Alonso, A. Lesarri, J. C. López and S. Mata, *Chem. Phys. Lett.* 2004, **392**, 1−6.

20) J. L. Neill, S. T. Shipman, L. Alvarez-Valtierra, A. Lesarri, Z. Kisiel and B. H. Pate, *J. Mol. Spectrosc*. 2011, **269**, 21-29.

21) M. J. Frisch et al., GAUSSIAN09, Gaussian, Inc., Wallingford CT, **2009**.

22) R. S. Ruoff, T. D. Klots, T. Emilson and H. S. Gutowski, *J. Chem. Phys.* 1990, **93**, 3142-3150.

23) H. M. Pickett, *J. Mol. Spectrosc.* 1991, **148**, 371-377.

24) J. K. G. Watson, In *Vibrational Spectra and Structure*; J. R. Durig, Ed.; Elsevier: New York/Amsterdam, 1977; Vol. 6, pp 1−89.

25) R. Meyer, *J. Mol. Spectrosc.* 1979, **76**, 266–300.

26) G. A. Jeffrey, An Introduction to Hydrogen Bonding, Oxford, 1997.

27) W. Caminati and Jens-Uwe Grabow, in Frontiers and Advances in Molecular Spectroscopy, chap. 17, Elsevier, 2018.

Graphical abstract: